# Characterization of UV pulses by plasma-mirror FROG using a liquid-sheet jet of water

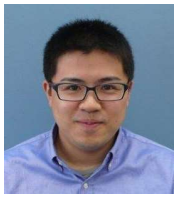

Tomoyuki Endo

Ultrafast Dynamics Group, Department of Advanced Photon Research

We have developed an all-optical technique based on time-resolved reflection spectroscopy to characterize ultrashort laser pulses [1–3]. Ultrafast switching of a plasma mirror formed by focusing near-infrared (NIR) intense laser pulses on a fused silica plate was used as a gate function in a frequency-resolved optical gating (FROG) trace. Since all the optics employed in this plasma-mirror FROG (PM-FROG) technique are reflective optics, pulse shapes can be characterized without requiring post-analysis to remove material dispersions. The PM-FROG technique was successfully applied to pulse characterization in the vacuum ultraviolet (VUV) region.

In previous studies, since a fused silica plate was employed as a target sample, the applicable repetition rate of the laser system was limited to 10 Hz by the speed of mechanical movement to avoid the effects of ablation damage on the target surface. In this study, we employ a liquid-sheet jet of water as a target instead of a solid to extend the applicable repetition rate to 1 kHz or more. The liquid-sheet jet provides an optically flat surface for each laser shot without mechanical operation of the target. Another concern was that the VUV waveform obtained by PM-FROG was not compared with one by another method. Here, we employ an ultraviolet (UV) pulse and compare the results obtained by PM-FROG and another established technique to demonstrate the validity of the PM-FROG technique.

The details of the experimental setup for producing a liquid-sheet jet were described elsewhere [4, 5]. Briefly, a peristaltic pump, a pulsation damper, and a slit-type nozzle are used to produce a flat-sheet jet of water with a flow rate of approximately 60 mL/min. The thickness of the liquid sheet is evaluated to be 8 μm by measuring the spectral interference between reflected UV pulses from the front and back surfaces. The output of a Ti:sapphire chirped pulse amplification system is introduced to a β-barium borate (BBO) crystal to generate the second-harmonic pulses. The residual fundamental NIR pulse and the second-harmonic UV pulse are separated by a dielectric mirror, which reflects the UV pulse and transmits the NIR pulse. The time delay between two pulses is controlled by a translational stage. The NIR and UV pulses are co-linearly combined again by another dielectric mirror and focused on the surface of the liquid-sheet jet of water by using a concave mirror with an effective focal length of 150 mm. Both NIR and UV pulses are horizontally polarized. A small incident angle of ~5° and a 4*f* image-relay setup are employed to reduce the effects of fluctuations in the orientation and curvature of the surface of the liquid-sheet jet due to residual pulsation of the pump. The spectra of the reflected UV pulse are recorded as a function of the time-delay $\tau$ between the NIR and UV pulses. The obtained FROG signal may be expressed as:

$$I_{sig}(\omega,\tau) = \left|\int_{-\infty}^{\infty} E(t-\tau)r(t)e^{-i\omega t}dt\right|^2,$$

where $\omega$ and $E(t)$ are the angular frequency and the complex electric field amplitude of the UV pulse, respectively, and $r(t)$ is the complex reflection coefficient of the plasma mirror.

The measured FROG trace is shown in Fig. 1(a). In the negative time-delay region where the UV pulse comes first, the contribution of the Fresnel reflection of unexcited water on the liquid-sheet surface is observed. The signal intensity decreases slightly and then increases dramatically. This indicates that the refractive index of the liquid-sheet surface is decreased as a result of plasma formation as described by the Drude model. Qualitatively speaking, the refractive index of water, $n_{\mathrm{water}}$, decreases and approaches that of air ($n_{\mathrm{air}} \approx 1$) as the plasma density increases, hence the reflection coefficient becomes zero. As the refractive index further decreases to $n_{\mathrm{water}} < 1$, the reflection coefficient begins to increase.

The least-squares generalized projections algorithm (LSGPA) [6] is adopted to reconstruct the FROG trace. To avoid convergence to a local minimum, the initial guess of the second-order dispersion of the UV pulse is obtained from the slope of the line along minimum values at each frequency component. When a Fourier-transform-limited pulse is radiated at a plasma mirror, all the frequency components are reflected simultaneously. This corresponds to a slope of zero. When a positively chirped pulse is reflected by a plasma mirror, the effective time-delay of each frequency increases as the frequency increases. As a result, the PM-FROG trace shows an earlier rise at a higher frequency. As shown in Fig. 1(a), the initial guess of the second-order dispersion is estimated to be −163 fs$^2$ from the slope.

The PM-FROG trace is successfully reconstructed by the LSGPA, as shown in Fig. 1(b). The retrieved temporal waveform and corresponding spectrum of the UV pulse are shown in Fig. 2. The full-width at half-maximum of the pulse duration is evaluated to be 52 fs by a Gaussian fit, which shows the pulse is almost

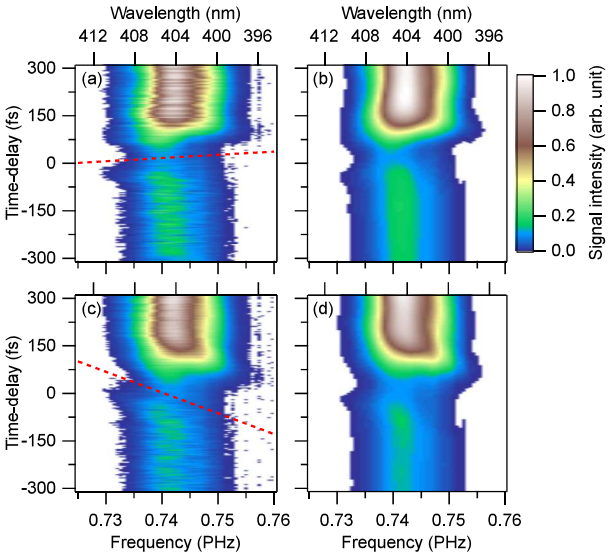


Fig. 1. (a) Measured FROG trace. The red dotted line is a linear fit for minimum values at each frequency in the FROG trace. (b) Reconstructed FROG trace by the LSGPA from (a). (c) Same as (a), but with the transmission of a fused silica plate (10 mm thick). (d) Same as (b), but from (c).

Fourier-transform-limited. The obtained spectrum is consistent with one measured by another spectrometer. Since there are no transmission optics in the PM-FROG setup, the PM-FROG technique would be applicable to pulse characterization of short-wavelength pulses without post-subtraction of material dispersions from the obtained phase.

To demonstrate pulse characterization of chirped pulses, a fused silica plate (10 mm thick) is introduced to add a chirp to the UV pulse. The measured FROG trace with the transmission of the fused silica plate is shown in Fig. 1(c). The slope of the red dotted line changes compared to that without the fused silica plate, showing that the PM-FROG trace reflects the second-order dispersion of the UV pulse as described above. The initial guess of the second-order dispersion for the chirped UV pulse is evaluated to be 1043 $fs^2$ from the slope. The reconstructed PM-FROG trace is shown in Fig. 1(d). The temporal waveform and corresponding spectrum of the chirped UV pulse are shown in Fig. 2. The pulse duration becomes longer than that without the fused silica plate and is estimated to be 60 fs. As shown in Fig. 2(b), the spectral phase shows a clear effect of the spectral dispersion by the fused silica plate. The second-order dispersions with and without the 10 mm fused silica plate are evaluated to be 903.5 ± 60.7 $fs^2$ and −61.7 ± 36.6 $fs^2$, respectively, by using a polynominal fit at the central frequency of 0.743 PHz. The group velocity dispersion (GVD) of fused silica is measured to be 96.5 ± 7.2 $fs^2$/mm.

Another established pulse characterization technique, SD-FROG, is also performed to demonstrate the validity of the results obtained by PM-FROG. A non-collinear SD-FROG setup is employed for a single-shot measurement in this study. In this SD-FROG setup, the UV pulse transmits a beam splitter (fused silica, 3 mm thick) to make a replica. Therefore, the second-order dispersion caused by the fused silica plate has to be subtracted from the retrieved spectral phase through post-analysis to obtain the actual waveform. The second-order dispersions measured by SD-FROG with and without the fused silica plate are evaluated to be 930.1 ± 207.7 $fs^2$ and 66.4 ± 215.3 $fs^2$, respectively, which are consistent with the values measured by PM-FROG within the error. The GVD of fused silica is evaluated to be 86.4 ± 29.9 $fs^2$/mm by SD-FROG.

The GVDs obtained by PM-FROG and SD-FROG are consistent with the value in the literature (96.2 $fs^2$/mm) of the GVD of fused silica [7]. These results indicate that PM-FROG can be used to characterize the waveform of the Fourier-transform-limited pulse, as well as of chirped pulses. The results by PM-FROG using the liquid-sheet jet of water are as reliable as the results by SD-FROG.

We demonstrated a pulse characterization technique based on time-resolved reflection spectroscopy for a high-repetition laser system. From the flow rate of the liquid-sheet jet, the applicable repetition rate of this technique would be extended to 100 kHz without a major update. By employing a liquid target instead of a solid target, the applicable repetition rate could be extended up to $10^4$ times. In addition, although we did not discuss this detail in this paper, the time-dependent complex reflection coefficient of the plasma mirror, $r(t)$, can be also retrieved from the PM-FROG trace. The PM-FROG technique would be a powerful tool not only to characterize a waveform, but also to investigate the plasma dynamics and ionization dynamics of a liquid.

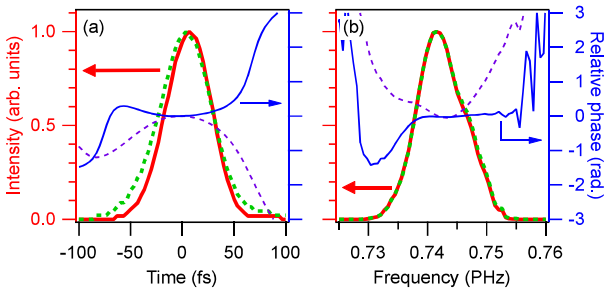


Fig. 2. (a) Temporal waveform and (b) corresponding spectrum of the UV pulse retrieved from Figs. 1(a) and (c) by the LSGPA. The dashed and solid lines correspond to the results with and without transmission of a fused silica plate (10 mm thick), respectively.

## Acknowledgments

The author thanks Drs. R. Itakura and M. Tsubouchi for their contributions, Drs. T. Nakajima and K. Nagashima for valuable discussion, and Y. Hagihara for technical support. This work has been supported by the following funding sources: Japan Society for the Promotion of Science (JSPS) (KAKENHI 17H02802); Research Foundation for Opto-Science and Technology; Ministry of Education, Culture, Sports, Science and Technology (MEXT) (Q-LEAP ATTO JPMXS0118068681); and Institute of Advanced Energy, Kyoto University (ZE30B-37).

## References

1. R. Itakura et al., Opt. Express **23**, 10914 (2015).
2. R. Itakura et al., High Power Laser Sci. Eng. **4**, e18 (2016).
3. R. Itakura et al., Opt. Lett. **44**, 2282 (2019).
4. M. Kondoh et al., Opt. Express **22**, 14135 (2014).
5. T. Endo et al., Opt. Lett. **44**, 3234 (2019).
6. J. Gagnon et al., Appl. Phys. B **92**, 25 (2008).
7. I. H. Malitson, J. Opt. Soc. Am. **55**, 1205 (1965).